JACS
JOURNAL OF THE AMERICAN CHEMICAL SOCIETY

COMMUNICATION

pubs.acs.org/JACS

Selective Biomolecular Nanoarrays for Parallel Single-Molecule Investigations

Matteo Palma,[*,†,‡] Justin J. Abramson,[‡] Alon A. Gorodetsky,[*,§] Erika Penzo,[†] Ruben L. Gonzalez, Jr.,[§] Michael P. Sheetz,[∥] Colin Nuckolls,[§] James Hone,[*,‡] and Shalom J. Wind[*,†]

Departments of [†]Applied Physics & Applied Mathematics, [‡]Mechanical Engineering, [§]Chemistry, and [∥]Biological Sciences, Columbia University, New York, New York, 10027, United States

Supporting Information

ABSTRACT: The ability to direct the self-assembly of biomolecules on surfaces with true nanoscale control is key for the creation of functional substrates. Herein we report the fabrication of nanoscale biomolecular arrays via selective self-assembly on nanopatterned surfaces and minimized nonspecific adsorption. We demonstrate that the platform developed allows for the simultaneous screening of specific protein−DNA binding events at the single-molecule level. The strategy presented here is generally applicable and enables high-throughput monitoring of biological activity in real time and with single-molecule resolution.

Nanoscale control over the organization of biomolecules at solid substrates is a powerful tool for addressing fundamental issues in many areas of biology.[1−9] Nanoarrays of biomolecules[10−18] can offer unmatched sensitivity, smaller test sample volumes in molecular diagnostics, and high-throughput analysis through the ability to monitor (distinct) biorecognition events in parallel on the same chip. By approaching the size scale of individual biomolecules, nanoscale control could conceivably allow us to carry out single-molecule investigations[19] (on an array) that in turn would enable monitoring of biochemical processes in real time, characterization of transient intermediates, and measurement of the distributions of molecular properties rather than their ensemble averages.[20,21] Key issues involved in developing a nanoscale biochip are related to the selectivity (and spot uniformity) of the biomolecular (self)assembly, the consequent minimization of nonspecific adsorption of the biomolecules under investigation, and the accessibility of recognition elements within an immobilized biomolecule.[22,23] All such issues affect signal-to-noise ratios and prevent proper interpretation of biomolecular binding/recognition events.[24,25]

Herein we present a strategy that overcomes all of the above limitations through control of the localization of biomolecules in ordered nanoarrays, allowing for high-throughput single-molecule investigations in real time. Specifically, we show how the dimensions and separation of the nanodots in the fabricated arrays allow for both clear addressability and parallel readout of single-molecule events of biological interest via conventional epifluorescence microscopy imaging. As a proof of principle, the activity of a DNA-binding enzyme, exemplified here by the restriction endonuclease PvuII, was monitored. This work highlights the clear advantage of true nanoscale confinement in the design of high-throughput (and high-resolution) heterogeneous assays for biological investigations.

For our studies, we began by nanopatterning a glass substrate surface via direct electron-beam lithography (EBL) to create 50 μm × 50 μm arrays of 30 ± 4 nm Au/Pd nanodots spaced 2 μm apart and interspersed with 500 nm registration squares spaced 10 μm apart (see Figures SI-1 and SI-2). Figure 1 shows the approach used to biofunctionalize the nanodots [details are given in the Supporting Information (SI)]. We first formed self-assembled monolayers (SAMs) of thiolated alkanes[26] exhibiting biotin headgroups. We next passivated the surface against nonspecific adsorption of biomolecules via the formation of a polyethylene glycol (PEG)−silane monolayer on the glass surface. Next, we immobilized streptavidin on the nanodots,[27,28] and finally, we tethered biotinylated DNA via a second biotin−streptavidin linkage.[29,30]

Epifluorescence microscopy imaging of the resulting array demonstrated the selectivity of the functionalization at the single-nanodot level. In particular, Figure 2a shows the immobilization of fluorescently labeled streptavidins on every nanodot, while Figure 2b shows the subsequent immobilization of fluorescently labeled double-stranded DNAs (dsDNAs). Each employed DNA molecule was labeled with one rhodamine red (RhodRed) fluorophore on the distal end of the duplex (i.e., on the end not attached to the surface-bound streptavidin). Furthermore, the uniformly passivated regions between the nanodots in Figure 2a,b exhibited a remarkably low fluorescence background and demonstrated the minimization of nonspecific adsorption achieved at the glass substrate. By measuring the average background fluorescence intensity of the glass surface before and after exposure of the substrate to fluorescently labeled DNA (see the SI and Figure SI-3), we were able to determine that the physisorbed DNA coverage on the glass surface of our biochip was 0.1−0.5 μm^{-2} (i.e., less than one DNA every 2 μm^2). It is noteworthy that because of the size of the nanodots and therefore the limited number of streptavidins and DNAs attached on each of them (see below for discussion), the ability to resolve single dots required the ultralow nonspecific adsorption that we achieved.[31]

To demonstrate the general suitability of our platform for monitoring biomolecular interactions, we carried out proof-of-principle restriction enzyme experiments on the functionalized

Received: February 1, 2011
Published: April 29, 2011

dx.doi.org/10.1021/ja201031g | J. Am. Chem. Soc. 2011, 133, 7656–7659

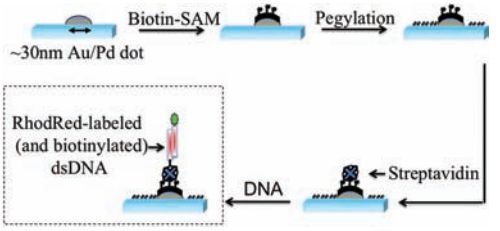

Figure 1. Scheme employed for the chemical functionalization of the nanopatterned substrate.

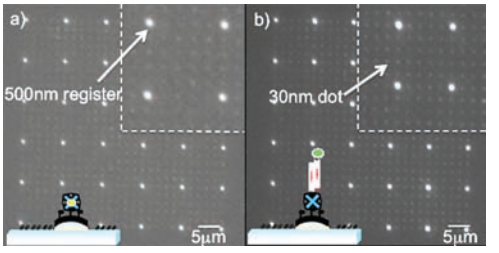

Figure 2. (a) Epifluorescence microscopy image of the electron-beam-written nanoarray functionalized with Alexa488-labeled streptavidins (100 ms exposure time). (b) Epifluorescence microscopy image of the nanoarray functionalized with RhodRed-labeled dsDNAs (100 ms exposure time). The insets at the top right-hand corners of (a) and (b) show zoomed fluorescence images of the corresponding arrays.

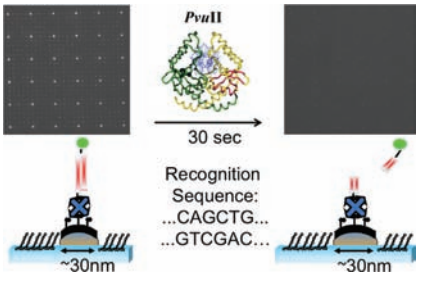

Figure 3. Scheme and epifluorescence microscopy images of PvuII recognition and cleavage of the nanodot-immobilized DNA (200 ms exposure times).

nanoarrays. We anchored to the surface of our nanoarray a 20 base pair (bp) DNA labeled with a RhodRed fluorophore (one fluorophore per DNA) on the distal end of the duplex (i.e., on the end not attached to the nanodot via the biotin−avidin linkage). The arrays were then incubated with PvuII-HF, a well-known and commercially available restriction enzyme with minimal star activity.[32] In the presence of the 5′-CAGCTG-3′ PvuII recognition site[33] on the employed DNA, we observed a complete loss of fluorescence intensity localized at the individual nanodots within seconds of addition of the enzyme (Figure 3). This is ascribable to DNA cleavage by the enzyme and consequent loss of the fluorescently labeled segment of the anchored DNA (see the scheme in Figure 3). Notably, no loss of localized fluorescence intensity at the nanodots was observed in the absence of the recognition site, consistent with a lack of DNA cleavage by PvuII (see Figure SI-4). Thus, the interaction of PvuII with the nanodot-immobilized DNA on our nanoarray was highly specific. This observation demonstrates that our platform is generally well suited for rapid, reliable, and specific real-time monitoring

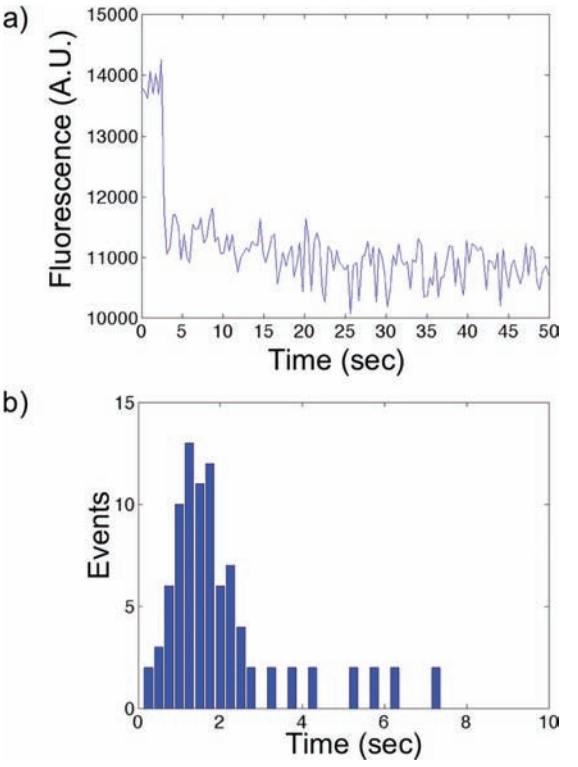

Figure 4. (a) Plot of the fluorescence intensity vs time for a representative single nanodot containing a single RhodRed-labeled DNA; the single-step loss of fluorescence intensity was derived from PvuII cleavage of the DNA (200 ms exposure time). (b) Representative histogram of single-molecule DNA cleavage events over an entire nanoarray.

of biomolecular interactions via conventional epifluorescence microscopy.

The minimized crowding of the immobilized DNA that arises from the nanoscopic size and microscopic spacing of the nanodots, in combination with the high selectivity and consequently high signal-to-noise ratio achieved, enabled us to obtain single-molecule resolution in monitoring the DNA−PvuII interaction. Each nanodot in our nanoarray was optically resolvable from its neighbors because of the 2 μm spacing, so we were able to monitor the loss of fluorescence at the single-nanodot level. This resulted in a loss of fluorescence intensity that occurred in discrete steps, as shown in Figure 4a. By extracting the time delay between when PvuII was first delivered to the nanoarray and when each single-DNA cleavage event was observed, we built a histogram of single-molecule fluorescence extinction as a function of time (Figure 4b).[34] It is noteworthy that the histogram is well-described by a difference of two exponentials (as shown in Figure SI-6); this implies the existence of at least two rate-determining steps in the PvuII−DNA cleavage reaction, consistent with the existence of a Michaelis−Menten complex.[35,36] In addition, our extrapolated value of the overall catalytic rate constant (i.e., the "turnover rate constant", k) for PvuII ($k \approx 1\ s^{-1}$) is comparable to previously reported values obtained from ensemble measurements under the same buffer conditions ($k \approx 0.3\ s^{-1}$).[37−39]

The discrete steplike drops in fluorescence intensity enabled us to determine the average number of DNA molecules immobilized on single nanodots.[40] Our analysis demonstrated that ~60% of the nanodots had one bound DNA molecule, ~20%

dx.doi.org/10.1021/ja201031g | J. Am. Chem. Soc. 2011, 133, 7656–7659

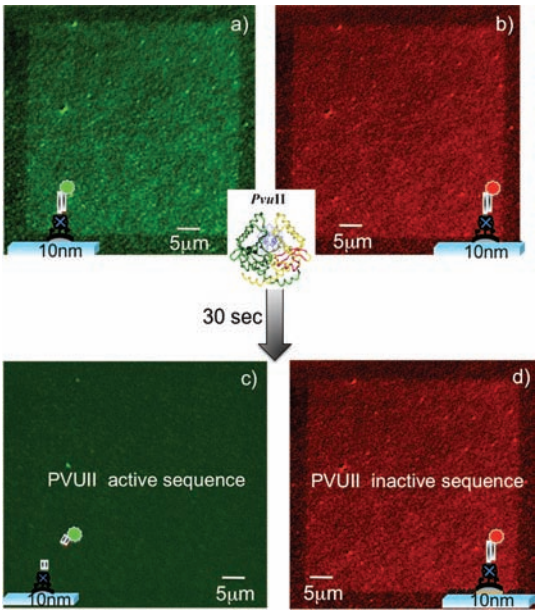

Figure 5. Epifluorescence microscopy images (100 ms exposure time) of the nanoimprinted nanoarray functionalized with RhodRed-labeled dsDNA exhibiting the PvuII recognition site (green channel) and Cy3-labeled dsDNA lacking the PvuII recognition site (red channel). (a, b) Images taken before addition of the enzyme. (c, d) Images showing that within seconds of the addition of the enzyme, the PvuII-active DNA is cleaved, as evidenced by the loss of fluorescence (green channel), while the PvuII-inactive DNA is not affected by the presence of the enzyme (red channel).

had two bound DNA molecules, and ~5% had three bound DNA molecules.[41] Although each 30 nm nanodot could accommodate up to ~30 streptavidins, each of which could anchor two biotinylated DNAs, we found fewer than four DNAs on ~85% of the nanodots. We postulate that this fortuitously sparse density of DNA results from a combination of an unfavorable arrangement of the streptavidins at the surface and electrostatic repulsion among DNA molecules during immobilization. In particular, the unknown arrangement that biotin−thiols adopt in a mixed SAM on a nanoscale substrate[42] is likely responsible for the limited number of streptavidins, and consequently DNAs, anchored on each nanodot.

In order to demonstrate that the process presented here is scalable, we monitored distinct biorecognition events on a single biochip that was fabricated using a low-cost nanopatterning technique. We coassembled two different 20 bp DNA molecules, one endonuclease-active and the other not, on a substrate patterned by nanoimprint lithography,[43] a lower-cost, higher-throughput patterning technique. The PvuII-active DNA was labeled with a RhodRed fluorophore, while the inactive DNA (i.e., lacking the PvuII recognition site) was labeled with a Cy3 dye molecule; in each case, the fluorophore was localized at the distal end of the duplex. We coassembled the DNAs on a 50 μm × 50 μm array of 10 ± 2 nm Au/Pd nanodots spaced 200 nm apart and fabricated by nanoimprint lithography[43] (see Figure SI-7).

Multichannel epifluorescence microscopy imaging of the resulting nanoarray enabled us to monitor the presence of the two different DNAs coassembled on the same nanoarray, as shown in Figure 5a,b: the RhodRed-labeled DNA was imaged in the green channel and the Cy3-labeled DNA in the red channel. The resulting nanoarray was then incubated with PvuII. Within seconds of the addition of the enzyme, we observed a loss of fluorescence for the PvuII-active DNA (green channel), as shown in Figure 5c. We attribute this to DNA cleavage by the enzyme and consequent loss of the fluorescently labeled segment of the anchored DNA, similar to that shown in Figure 3. Notably, no loss of fluorescence intensity was observed on the same nanoarray for the DNA lacking the PvuII recognition site and labeled with the Cy3 fluorophore (red channel; see Figure 5d), consistent with a lack of DNA cleavage by the enzyme. This proves that our platform allows simultaneous monitoring of two distinct biorecognition events on the same biochip (patterned via a low-cost fabrication technique).

In summary, we have demonstrated the ability to control the immobilization of biomolecules at surfaces in arrayed 30 nm domains, minimizing nonspecific adsorption and allowing for the parallel monitoring of specific protein−DNA binding events at the single-molecule level. This also allowed us to determine the average number of DNA molecules immobilized on single 30 nm dots: we found fewer than four DNAs on ~85% of the nanodots. Notably, the overall strategy is highly general and can be utilized to immobilize any biotinylated biomolecule for further studies. By specific design of the biomolecular nanoarray, conventional epifluorescence microscopy imaging can be used to record hundreds of single-molecule events of biological interest simultaneously on a single biochip; to our knowledge, this is the first time biological activity has been monitored on a nanoarray with such high density and resolution (i.e., single-molecule investigations carried out in parallel). Furthermore, the fabrication strategy can be easily scaled via nanoimprint lithography, a lower-cost, higher-throughput patterning technique. In this context, we have also shown that we can fabricate and biofunctionalize arrays of ~10 nm domains and that we can dynamically monitor distinct biorecognition events on the same biochip. We envision that the high density and resolution achievable with our platform will find general application in high-throughput heterogeneous assays of a wide variety of biomolecular interactions.

■ ASSOCIATED CONTENT

Supporting Information. Experimental procedures, nanofabrication, surface functionalization, fluorescence microscopy, AFM images, scanning electron microscopy images, single-molecule data for physisorbed DNA, control enzyme experiments, bleaching data, the single-molecule fitted histogram, and complete ref 18. This material is available free of charge via the Internet at http://pubs.acs.org.

■ AUTHOR INFORMATION

Corresponding Author
mp2766@columbia.edu; ag2909@columbia.edu; jh2228@columbia.edu; sw2128@columbia.edu

■ ACKNOWLEDGMENT

We gratefully acknowledge support from the Office of Naval Research under Award N00014-09-1-1117, the National Institutes of Health through Award PN2EY016586 under the NIH Roadmap for Medical Research, and the National Science Foundation under Award NSF EF-05-07086. Additional support from the Nanoscale Science and Engineering Initiative of the

National Science Foundation under NSF Award CHE-0641523 and from the New York State Office of Science, Technology, and Academic Research (NYSTAR) is also gratefully acknowledged. This work was also supported by the National Science Foundation under Award CHE-0936923.

REFERENCES

(1) Stephanopoulos, N.; Solis, E. O. P.; Stephanopoulos, G. *AIChE J.* **2005**, *51*, 1858.
(2) Langer, R.; Tirrell, D. A. *Nature* **2004**, *428*, 487.
(3) Rosi, N. L.; Mirkin, C. A. *Chem. Rev.* **2005**, *105*, 1547.
(4) Torres, A. J.; Wu, M.; Holowka, D.; Baird, B. *Annu. Rev. Biophys.* **2008**, *37*, 265.
(5) Wong, L. S.; Khan, F.; Micklefield, J. *Chem. Rev.* **2009**, *109*, 4025.
(6) *Nanobiotechnology*; Wiley-VCH: Weinheim, Germany, 2004.
(7) Aydin, D.; Schwieder, M.; Louban, I.; Knoppe, S.; Ulmer, J.; Haas, T. L.; Walczak, H.; Spatz, J. P. *Small* **2009**, *5*, 1014.
(8) Niwa, D.; Omichi, K.; Motohashi, N.; Homma, T.; Osaka, T. *Chem. Lett.* **2004**, *33*, 176.
(9) Zhang, G. J.; Tanii, T.; Zako, T.; Hosaka, T.; Miyake, T.; Kanari, Y.; Funatsu, T. W.; Ohdomari, I. *Small* **2005**, *1*, 833.
(10) Nicolau, D. V.; Demers, L.; Ginger, D. S. In *Microarray Technology and Its Applications*; Nicolau, D. V., Müller, U. R., Eds.; Springer: Berlin, 2005; pp 89−118.
(11) *Nanobiotechnology II*; Wiley-VCH: Weinheim, Germany, 2007.
(12) Bulyk, M. L.; Gentalen, E.; Lockhart, D. J.; Church, G. M. *Nat. Biotechnol.* **1999**, *17*, 573.
(13) Demers, L. M.; Ginger, D. S.; Park, S. J.; Li, Z.; Chung, S. W.; Mirkin, C. A. *Science* **2002**, *296*, 1836.
(14) Bruckbauer, A.; Ying, L. M.; Rothery, A. M.; Zhou, D. J.; Shevchuk, A. I.; Abell, C.; Korchev, Y. E.; Klenerman, D. *J. Am. Chem. Soc.* **2002**, *124*, 8810.
(15) Rodolfa, K. T.; Bruckbauer, A.; Zhou, D. J.; Korchev, Y. E.; Klenerman, D. *Angew. Chem., Int. Ed.* **2005**, *44*, 6854.
(16) Huang, S. X.; Schopf, E.; Chen, Y. *Nano Lett.* **2007**, *7*, 3116.
(17) Akbulut, O.; Jung, J. M.; Bennett, R. D.; Hu, Y.; Jung, H. T.; Cohen, R. E.; Mayes, A. M.; Stellacci, F. *Nano Lett.* **2007**, *7*, 3493.
(18) Drmanac, R. et al. *Science* **2010**, *327*, 78.
(19) Ishijima, A.; Yanagida, T. *Trends Biochem. Sci.* **2001**, *26*, 438.
(20) Ritort, F. *J. Phys.: Condens. Matter* **2006**, *18*, R531.
(21) Smiley, R. D.; Hammes, G. G. *Chem. Rev.* **2006**, *106*, 3080.
(22) Houseman, B. T.; Mrkisch, M. *Angew. Chem., Int. Ed.* **1999**, *38*, 782.
(23) Castronovo, M.; Radovic, S.; Grunwald, C.; Casalis, L.; Morgante, M.; Scoles, G. *Nano Lett.* **2008**, *8*, 4140.
(24) Bulyk, M. L. *Adv. Biochem. Eng. Biotechnol.* **2007**, *104*, 65.
(25) Field, S.; Udalova, I.; Ragoussis, J. *Adv. Biochem. Eng. Biotechnol.* **2007**, *104*, 87.
(26) Love, J. C.; Estroff, L. A.; Kriebel, J. K.; Nuzzo, R. G.; Whitesides, G. M. *Chem. Rev.* **2005**, *105*, 1103.
(27) Cherniavskaya, O.; Chen, C. J.; Heller, E.; Sun, E.; Provezano, J.; Kam, L.; Hone, J.; Sheetz, M. P.; Wind, S. J. *J. Vac. Sci. Technol., B* **2005**, *23*, 2972.
(28) *Avidin−Biotin Technology*; Wilchek, M., Bayer, E. A., Eds.; Methods in Enzymology, Vol. 184; Academic Press: San Diego, CA, 1990.
(29) Ladd, J.; Boozer, C.; Yu, Q. M.; Chen, S. F.; Homola, J.; Jiang, S. *Langmuir* **2004**, *20*, 8090.
(30) Smith, C. L.; Milea, J. S.; Nguyen, G. H. *Top. Curr. Chem.* **2005**, *261*, 63.
(31) Indeed, when the metal thiolation step in the functionalization process was performed after the PEG−silane step, we observed that the biotin−thiols physisorbed on the PEG surrounding the nanodots and functioned as anchoring points for streptavidin and consequently for the DNAs, thus increasing the background fluorescence and preventing the resolution of single nanodots via epifluorescence microscopy imaging.
(32) Available from New England Biolabs. See: http://www.neb.com/nebecomm/products/productR3151.asp (accessed Feb 1, 2011).
(33) Athanasiadis, A.; Vlassi, M.; Kotsifaki, D.; Tucker, P. A.; Wilson, K. S.; Kokkinidis, M. *Nat. Struct. Biol.* **1994**, *1*, 469.
(34) Photobleaching occurred at a rate that was more than 1 order of magnitude lower than the rate of PvuII cleavage (Figure SI-5). This allowed us confidently to dismiss photobleaching in our single-molecule enzyme data.
(35) Lu, H. P.; Xun, L. Y.; Xie, X. S. *Science* **1998**, *282*, 1877.
(36) Xie, S. N. *Single Mol.* **2001**, *2*, 229.
(37) Xie, F. Q.; Dupureur, C. M. *Arch. Biochem. Biophys.* **2009**, *483*, 1.
(38) Xie, F. Q.; Qureshi, S. H.; Papadakos, G. A.; Dupureur, C. M. *Biochemistry* **2008**, *47*, 12540.
(39) Simoncsits, A.; Tjornhammar, M. L.; Rasko, T.; Kiss, A.; Pongor, S. *J. Mol. Biol.* **2001**, *309*, 89.
(40) This was done by counting the number of discrete steplike drops in the fluorescence intensity versus time for trajectories arising from both PvuII activity (on PvuII-treated nanoarrays) and photobleaching (on untreated nanoarrays).
(41) The remaining ∼15% of the nanodots lacked discrete steplike drops in fluorescence intensity and instead exhibited a relatively continuous decay likely arising from a large density of immobilized DNAs, thus preventing single-molecule resolution.
(42) Jackson, A. M.; Myerson, J. W.; Stellacci, F. *Nat. Mater.* **2004**, *3*, 330.
(43) Schvartzman, M.; Wind, S. J. *Nano Lett.* **2009**, *9*, 3629.